Observations of Electric Fields Near the Plasmapause at Midnight

R. C. OLSEN

University of Alabama, Huntsville

T. L. AGGSON AND B. G. LEDLEY

NASA Goddard Space Flight Center, Greenbelt, Maryland

We report here static electric field measurements in the equatorial plane from the 100-m double floating probe experiment carried on the SCATHA (P-78-2) satellite. Eclipse measurements on auroral L shells are studied to better understand the change in magnetospheric convection at the plasmapause. The use of eclipse data allows the electric fields to be measured directly without contamination from the spacecraft photoelectron sheath; and it allows the thermal ion population in the outer plasmasphere to be observed, identifying the satellite location with respect to the plasmapause. (Such measurements are limited to near local midnight.) We find that in the corotating frame there is generally an electric field component in the antisolar direction during periods of low magnetic activity which begins at the edge of the plasmasphere and builds in amplitude as the satellite enters the plasma sheet. The amplitude of this electric field varies from 0.05 mV/m to 0.2 mV/m with increasing magnetic activity; the electric field switches to radially inward during periods of high activity with magnitudes up to 2 mV/m. The amplitude of the observed electric field increases with the amount of contribution from east-west currents in the earth's plasma sheet—magnetotail current system. Since the electric fields observed on these eclipse passes are radially outward in the midnight meridian during periods of low activity and since they are observed on a near-synchronous satellite which generally corotates with the earth, they are not included in most modeling studies of the formation of the plasmasphere.

INTRODUCTION

Electric Fields

There is near-general agreement in the literature that convection electric fields in the magnetosphere will play a role in the formation of the plasmapause. There are, however, no published direct electric field measurements in the literature correlating changes in the convection fields with changes in the plasma structure at the plasmapause. We will discuss here in-situ measurements of static electric fields at the plasma-pause as measured on the SCATHA satellite.

The role of electric fields in the structure of the plasma-sphere is a topic of considerable interest. The origin of the electric field patterns at the plasmapause is generally expected to be from three separate sources: (1) the general dawn-todusk-oriented magnetospheric electric field pattern produced by interaction of the solar wind and magnetosphere at the magnetopause, (2) the charge separation produced by particle drifts, at the edge of the plasma sheet which is generally referred to as the Alfven layer and which is expected to produce shielding of the plasmasphere from the general magnetospheric electric field, and (3) the corotation field which is the result of the expected corotation of the inner magnetosphere as a result of the high conductivity of the plasma along magnetic field lines anchored to the corotating ionosphere.

These three electric field systems should interact at the plasmapause such that the radial electric field would be a strong function of the gradient in the electron density (see review by Wolf [1975]). For the most part it is expected that the plasma-sphere should corotate with the earth during periods of low magnetic activity. Direct measurements of electric fields in the equatorial

magnetosphere, although still sparse, are becoming available for plasmasphere modelers. Double floating spherical probe measurements from the GEOS 1 satellite have been reported by *Pedersen et al. [1978], Pedersen and Grard [1979], and Pedersen et al. [1984]*. During periods of average Kp indexes they have reported variable electric fields with an average dawn-dusk magnitude of 3 mV/m at L values from 5 to 7. These magnitudes would average to an unreasonably large cross-magnetosphere potential, so these observers suggested that these observations may be due to local inhomogeneities. During quiet periods, variations of several millivolts per meter were common, but the average electric fields were less than 1 mV/m.

More recently, *Maynard et al. [1983]* have derived complete 24-hour plots of plasmasphere electric fields from observations made with the cylindrical electric field probes carried on the ISEE 1 satellite. These authors showed that the auroral electric fields (type 1 above) regularly penetrated into the corotating plasmasphere with increasing magnetic activity, with magnitudes from 1 to 2 mV/m.

Beyond the plasmapause there are no general survey studies published from direct electric field measurements in the equatorial magnetosphere. *Mcllwain [1972]* has modeled the motions of plasma clouds at synchronous orbits. This model provides information on the global fields, but less on the detailed screening of the type 1 electric fields by the plasmasphere in the immediate vicinity of the plasmapause.

The electric fields to be reported in the present paper are not available for 24-hour survey coverage; they are confined to eclipse periods in the region of local midnight at L = 5–7. However, we are able to correlate in detail the variation of the radial electric fields with plasma density at the plasmapause during periods of low magnetic activity when the satellite is in eclipse. These observations are a useful background to under-standing the reliability of the electric field technique. The main contribution to be made here, however, is the actual profile of the radial electric field at the plasmapause.
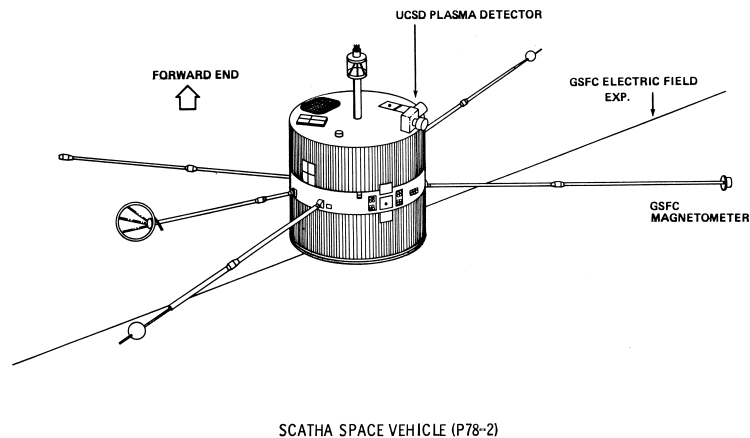
SCATHA SPACE VEHICLE (P78-2)

Fig. 1. Schematic drawing of P-78-2 SCATHA satellite, which was launched into a near-synchronous orbit in January 1979. The electric field sensors are each 50 m in length and are 0.64 cm (¼ inch) in diameter. The inner 30 m of each antenna is coated with Kapton (an insulator) to remove the active area of the floating potential probes from the photoelectron sheath of the satellite.

The studies to be presented of the electric field at the terminator of the plasmapause are unique because of the difficulty of this type of experiment at low plasma densities. There have been a number of recent satellite missions which carried electric field probe experiments through this region of the magnetosphere *[Pedersen et at., 1978; Mozer et al., 1978; Heppner et at., 1978a, b; Pedersen et al., 1984]*. All these experiments have been unable, so far, to accurately monitor the electric field profile at the plasmapause because of errors introduced by photoelectron emission at low plasma densities. A portion of this present paper on SCATHA electric field measurements will relate to measurements made in the sunlight.

Plasmapause Definition

The plasmapause is defined as the outer boundary of the plasmasphere, and as such it is found to be the outer boundary for cold, iosotropic plasma. It has also been identified as a density gradient, or the 10-100 cm-3 density contour. Such a definition was originally made by *Carpenter [1966],* on the basis of whistler data. The same definition is useful for plasma-pause determinations using thermal plasma data, such as that from OGO 5, where it was found that the sharp gradient typically coincided with the 100 cm-3 boundary, though at local midnight, 10 ions cm^{-3} seemed more appropriate *[Chappell et al., 1970]*. The latter definition is close to that used by *Taylor et al. [1968]* in interpreting OGO 1 and OGO 3 data. Use of the saturation characteristics of the Explorer 45 electric field antenna produced a working definition of 60 cm^{-3}, in association with sharp density gradients *[Maynard and Grebowsky, 1977]. Theoretically,* the plasmapause has traditionally been associated with the outermost closed particle trajectories, i.e., drift paths that are essentially corotating *[Kavanagh et at., 1968]*. This might also be considered the inner edge of the plasma sheet. Note that this definition requires steady state electric fields, which may be unrealistic. The con-junction of the inner edge of the plasma sheet with the plasmapause is not guaranteed in general, but at local

midnight they are generally coincident *[Horwitz et at., 1982]*. In this work, the inner edge of the plasma sheet is taken as the plasmapause, along with the transition from warm anisotropic (field-aligned) to cold isotropic ions.

Satellite and Instruments

The P-78-2 (SCATHA) satellite shown in Figure 1 was launched into a near-synchronous orbit in late January 1979, as part of a joint NASA/Department of Defense program to study spacecraft charging at high altitudes. The SCATHA orbit is elliptical, ranging from 5.3 to 7.7 RE, with a period of 23.5 hours, and with an inclination of 7.8° to the equatorial plane. The satellite spin period is 59 s, with the spin axis perpendicular to the earth-sun line. Although the satellite was not conducting, the concern of the SCATHA program and satellite with charging and the extensive analysis of the satellite's charging characteristics
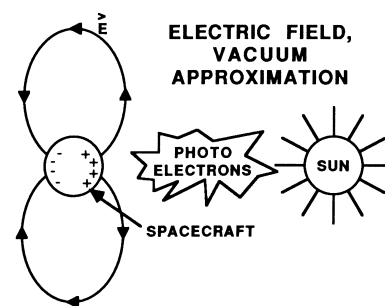

Fig. 2. Schematic of satellite and photoelectron cloud, which results in a sunward electric field.
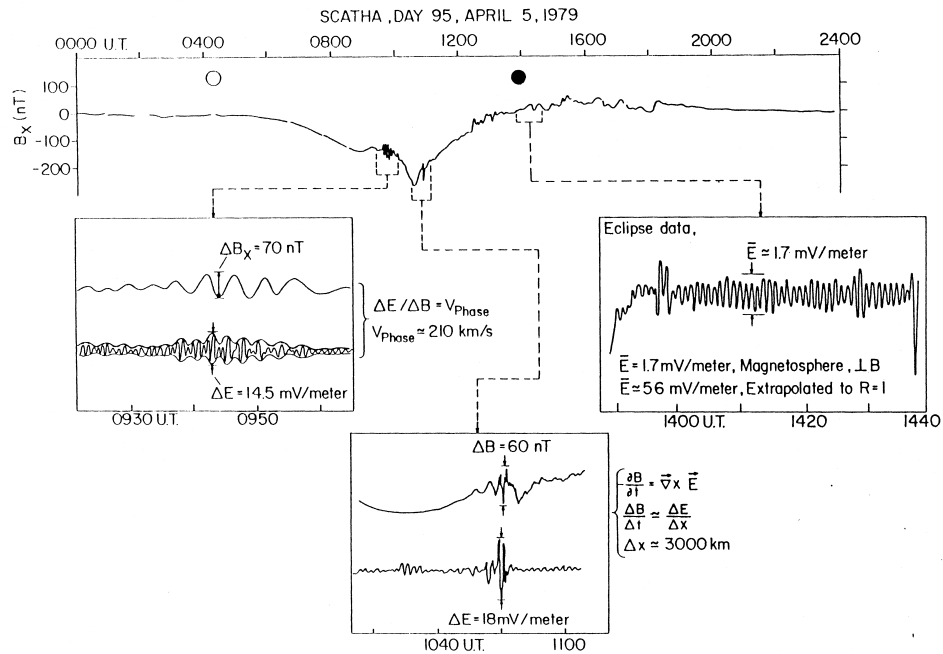
Fig. 3. Electric fields encountered during the 24-hour period of day 95, 1979. The electric field data are plotted in spacecraft coordinates to show the sine wave nature of the observations. Large (~ 7.5 mV/m) electric fields associated with a Pc 5 wave were observed at ~ 1000 UT. A transient electric field (~ 9 mV/m) is associated with a substorm onset observed at 1050 UT. A much smaller (~ 1.7 mV/m) electric field was observable during the spacecraft eclipse period because of the improved accuracy of the experiment in eclipse.

aids in understanding the electric field measurements. The satellite is eclipsed for roughly 1-hour periods for 40 days around the spring and fall equinoxes, providing electric field data free from photoelectron contamination.

The Goddard Space Flight Center (GSFC) electric field experiment consists of two 50-m antennas projecting into the spin plane. The cylindrical double floating probes are insulated for 30 m, providing an 80-m baseline. The minimum measurable field is 0.05 mV/m. Although the time resolution of the field measurements is limited by the satellite spin period, particularly in comparison to the ISEE 1 satellite, this satellite provides a compensating advantage. The $V \times B$ corrections due to the satellite motion are negligible because of the nearly geosynchronous orbit.

Two other instruments are used for this study. Particle data from the University of California, San Diego (UCSD) electrostatic analyzers (ESA) are used to identify the spacecraft location, e.g., plasmasphere, plasmapause, or plasma sheet, and to determine if the satellite has charged substantially negative ($\phi_{s/c} < -10$ V), while magnetic field data from the GSFC magnetometer show the deformation of the magnetic field from quiet conditions.

The UCSD particle detectors consist of five ESAs arranged in two rotating pairs of electron and ion detectors, and one fixed ion detector. One of the pairs of rotating detectors covers the energy range from 1 eV to 81 keV, while the other pair and the fixed ion detector cover the 1-eV to 1800-eV energy range. They are differential in energy ($\Delta E/E \sim 20\%$) and angle ($5° \times 7°$) and require 16 s for a complete energy scan. The instrument has been more fully described by Mauk and McIllwain [1975].

The GSFC magnetometer is a triaxial flux gate magnetometer mounted on a 4-m boom. The resolution is 0.3 y, with four vector measurements per second.

Photoelectron Effects

In order to understand the principal limitations on the ac-curacy of the electric field experiment it is important to consider in some detail the results of the photoemission from the main body of the SCATHA spacecraft. If the charge density of the photoelectron cloud emitted from the sunlit portion of the spacecraft is neglected, this portion of the spacecraft surface would charge positive, and the electrostatic perturbation produced by the spacecraft would present an error field orientated antisunward as a result of the Green's function contribution to the electrostatic potential. Actually, beyond a distance of several meters from the spacecraft the photoelectron cloud shown in Figure 2 seems to dominate the errors in the electric field experiment [Aggson et al., 1983a], and the error fields are predominantly in the sunward direction. In addition to a general sunward component of the electric field in the satellite photoelectron sheath, the random electron current from the photoelectron cloud is unbalanced on the sunward side, which contributes to a nonsinusoidal waveform which is a readily evident signature of systematic errors from the satellite sheath; sheath error free data have a pure sinusoidal wave-form (see Figure 22). During periods of low magnetic activity the data from the electric field
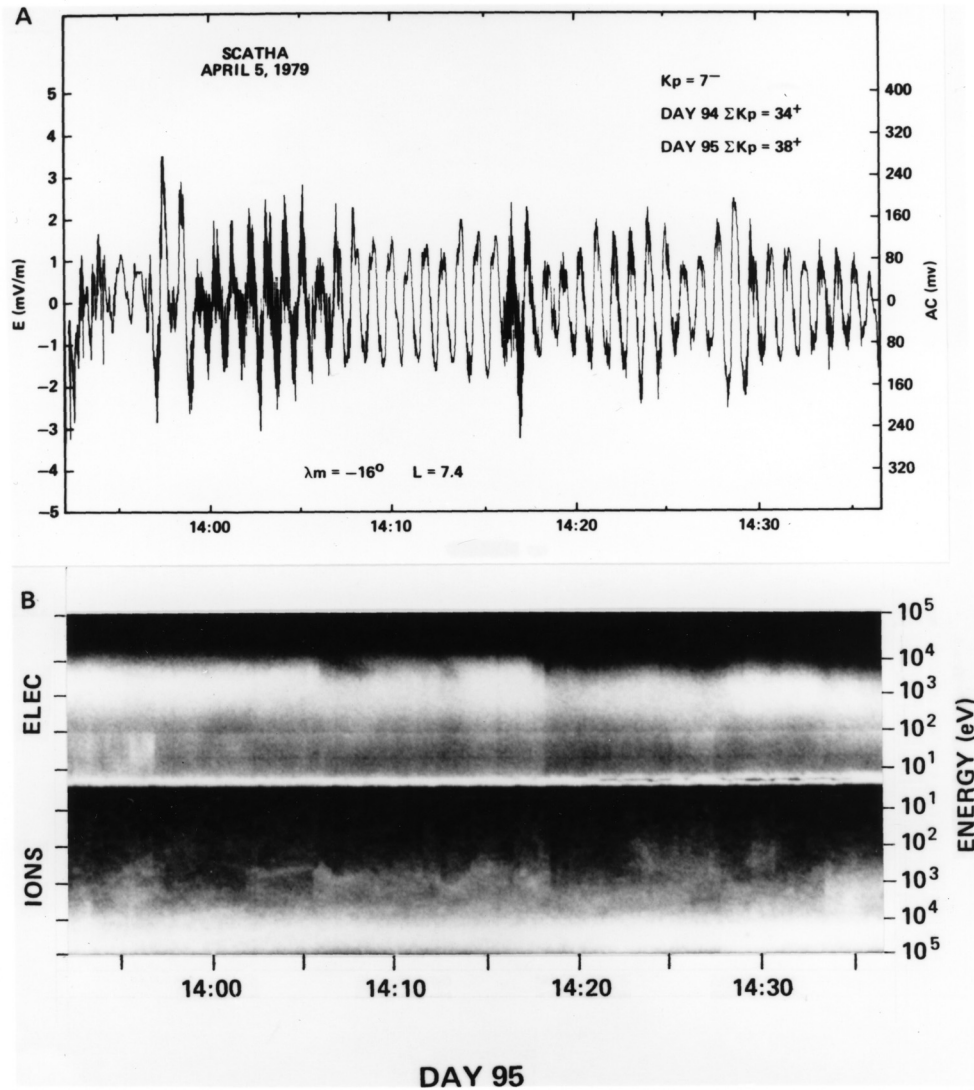
Fig. 4. (a) Further resolution of the eclipse data from day 95, 1979. The large excursions in the observed electric field on entering and leaving the eclipse period are due to thermal shock of the electric field probes, which causes a lack of the required alignment between opposing probes. Kp was 7+ during this period. The observed (sunward) electric field at -15° magnetic latitude projects to a northward field in the southern hemisphere/ionosphere. The satellite is outside the plasmasphere in the region of the plasma sheet. (b) Particle data for day 95 of 1979. Electron data are shown in the top panel, and ion data in the bottom panel. The energy axes both begin with zero energy at the center, with electron energy increasing upward, and ion energy increasing downward. These are the two high-energy detectors, with energy ranges for 0-81 keV. The count rate is coded as a gray scale, with zero counts (or background) plotted as black and high count rates plotted as white. The gray scale cycles back to black for the high fluxes of low-energy electrons seen in sunlight (photoelectrons).

experiment suffer seriously from such sheath overlap errors, with magnitudes from 1 to 5 mV/m in the sunward direction and from 0.5 to 2 mV/m perpendicular to the earth-sun line. The cylindrical shape of the sensors can also induce errors due to illumination variations, but this is a small effect for the differential (probe-to-probe) measurement.

These sheath signals decrease substantially as the ambient plasma density increases. At densities of 50 cm-3 or higher, quiet time electric fields of 0.2 to 0.8 mV/m were measured by the long electric antenna on ISEE 1. Similar measurements are possible with the SCATHA instrument in the plasmasphere, particularly the dusk bulge, though the longer antenna of the ISEE 1 satellite (179 m baseline as compared to the 80-m
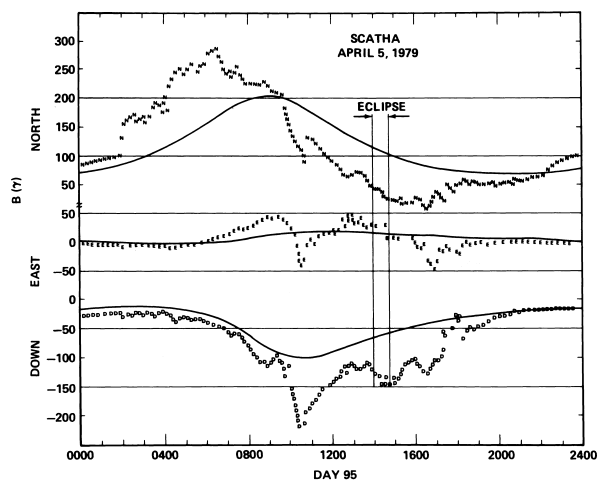
Fig. 5. SCATHA magnetic field plot for day 95, 1979. The magnetic field has been averaged over 1-min periods. The three components of B are in topographic coordinates where X is northward, Y is eastward, and Z is downward through the center of the earth. This was a magnetic storm day beginning with a sc at 0150 UT. At the time of the eclipse, 1345 to 1445, the magnetic field at the satellite in the midnight meridian was highly distorted from a dipole configuration, as can be seen by comparing the data with dipole solutions (solid lines).

SCATHA baseline) and electrostatic cleanliness of the ISEE 1 satellite allow for greater sensitivity. One example of eclipse data from ISEE 1 is shown by *Heppner et al. [1978b],* in their Figure 7.

Since the boundary of the plasmasphere and plasma sheet typically represents a drop in density from over 100 cm—3 to less than 10 cm-3, variations in electric fields across the density gradient would normally be masked by variations in the sunward field due to photoelectrons. The measurements obtained in eclipse with SCATHA therefore form a unique complement to the ISEE 1 plasmasphere observations.

The one limitation to the use of eclipse data is that if the plasma becomes hot enough, the satellite (and antenna) charges negatively. This typically happens if the ambient electron energy exceeds 10 keV [*Olsen, 1983*]. Such events were excluded from this study.

As mentioned above, the SCATHA satellite is spinning roughly in the X-Z plane at a spin rate of 1 rpm (see Figure 18). Most electric field experiments Fourier analyze the volt-age induced on the spinning antenna to yield two components of the electric field vector in the spin plane. Because of the very low spin rate on the SCATHA satellite, many geophysical time dependent fields are best surveyed in a raw data mode, i.e., in the spinning spacecraft coordinate system. When the SCATHA data are despun, the solar ecliptic (SE), or geocentric solar ecliptic (GSE), reference system is normally chosen. (Actually, it is a satellite-centered system parallel to the earth-oriented axes.) The SE X axis points from the earth toward the sun, while the Y axis is chosen to be in the ecliptic plane pointing toward dusk. The Z axis is perpendicular to the ecliptic plane. The satellite spin axis is maintained approximately perpendicular to the X-Z plane and in the orbit plane. There are no electric field data measured along the SE Y (or spin) axis. The resulting measurements are essentially the radial component of the equatorial field. The transformation from the measured fields to the

ambient fields requires theaddition of a 0.3-mV/m sunward field to account for the satellite motion.

The electric field data which follow will show one set of daylight data during a period of large electric fields and then progress from periods of high magnetic activity to quiet times at the plasmapause.

OBSERVATIONS

Sunlight—High Magnetic Activity

Figure 3 shows a set of data from a magnetically disturbed day on April 5, 1979. The spin axis (or SE Y) component of the magnetic field vector is plotted on top of Figure 3 to link the three different types of quasi-static electric fields which are evident during this 24-hour period. In the box to the left, the electric field and magnetic amplitudes of a Pc 5 magnetospheric oscillation are readily evident above the experimental noise. Similar Pc 5 oscillations have been shown by *Pedersen et al. [1978]* from GEOS 1. Electric field measurements on ISEE of Pc 1 and Pc 3 oscillations have been reported by *Moe et al. [1980].* In the center box of Figure 3, a large 18-mV/m transient electric field event was observed at 1900 MLT in coincidence with an auroral breakup event. The ratio of E(t) and dB/dt can be used from this event to estimate the scale size of the current system involved in this event which involves both field-aligned and ring current systems [*Aggson et al., 1983b].*

More relevant to this paper on plasmapause structure, the box on the right of Figure 3 shows the eclipse data measured on this day. Here, the photoelectron sheath which contaminates this experiment has vanished with the extinction of the solar radiation in the eclipse, and much smaller electric fields are resolvable. The electric field amplitude was surprisingly steady during this period, running from 1 to 2 mV/m in the sunward direction. Such a convective electric field maps to a southward electric field in the northern hemisphere of about 56 mV/m in the auroral ionosphere. The large convectional flows observed during this period are clearly due to the auroral electric field which we have called type 1 electric fields in the introduction. The plasma data in Figure 4b indicate that the satellite was beyond the plasmapause and in the plasma sheet region during this period.

Eclipse Electric Fields in the Plasma Sheet

The eclipse data from day 95, 1979, are shown again in Figure 4a with better resolution for comparison with the examples which follow. The magnetic field vector during the eclipse period of day 95 was highly disturbed (Kp = 7) during the eclipse period, as can be seen in Figure 5, where B is plotted in topographic Cartesian coordinates. Solid curves corresponding to components of a model dipole field are also plotted. The magnetic field was highly distorted from a dipole configuration during the eclipse measurements. The distortion of the magnetic field can be quantified for day 95 as $|\Delta B| = [(\mathbf{B}_{meas} - \mathbf{B}_{dipole})/|\mathbf{B}_{dipole}|$, with a value of 1.04. The interplanetary magnetic field was northward, with a value of 25 γ. The satellite was in the plasma sheet, and the plasma was convecting eastward with a relatively high $\mathbf{E} \times \mathbf{B}/B^2$ convective velocity (~10 km/s). Figure 4b shows that plasma sheet electrons extend up to 10 keV. This indicates that the local Alfven layer, or drift energy boundary, is associated with that energy [see *DeForest and McIlwain, 1971; Olsen, 1983*]. This spatial boundary is related to the intensity of the convection electric fields, on a global scale, and we will see that the local measurement made by SCATHA reflects the global fields.
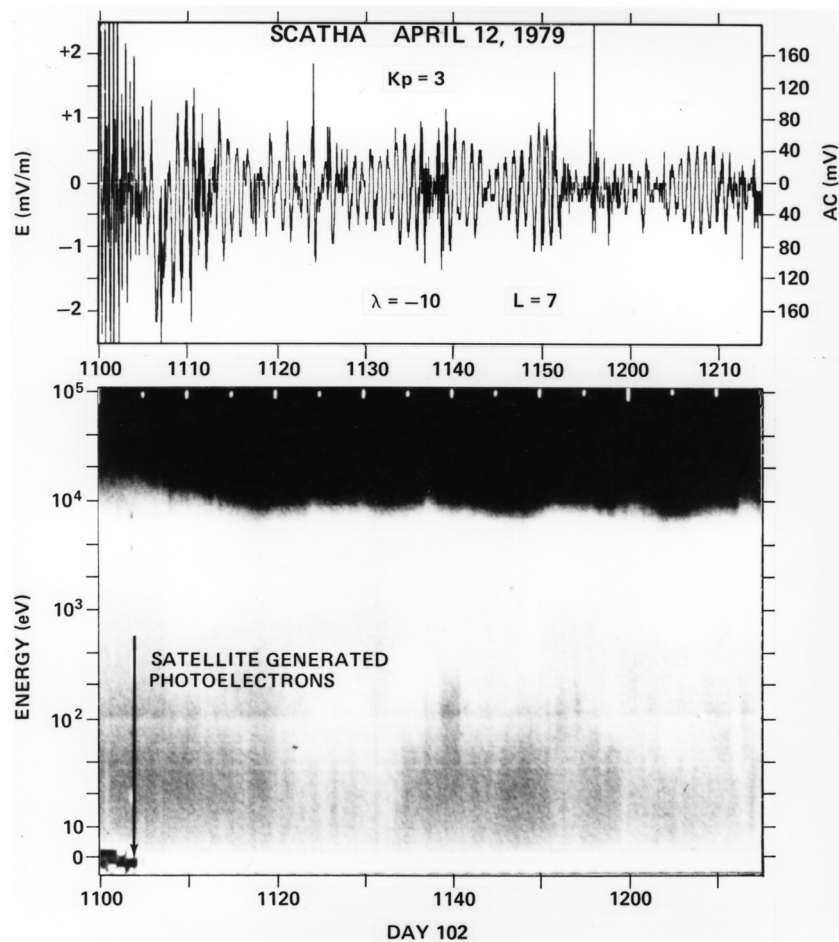
Fig. 6. (Top) Electric field data for day 102, 1979. The eclipse is from 1105 to 1215. The electric field varies from 0 to 1 mV/m. (Bottom) The particle data show electrons up to 10 keV, with some modulation of the boundary. Only the high-energy electrons are shown.
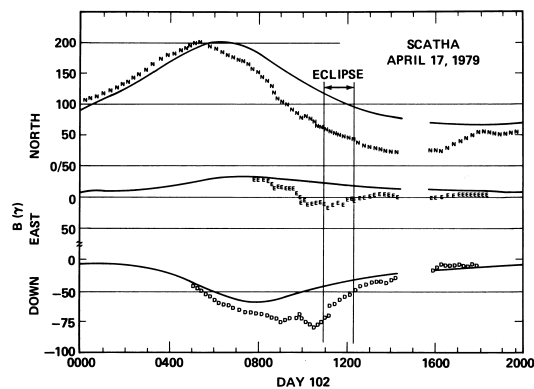
Fig. 7. Magnetic field components for day 102, 1979, in topographic coordinates. The magnetic field is distorted from a dipole configuration at the time of the eclipse, but this distortion is less than that shown for day 95.
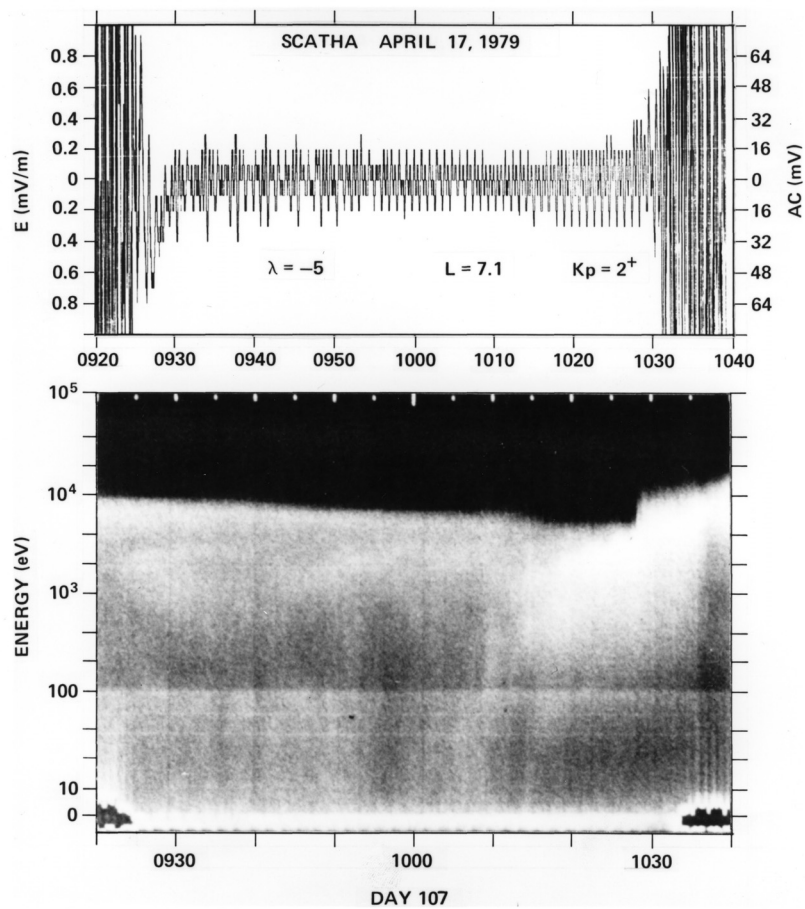
Fig. 8. (Top) Electric field data for day 107, 1979. The eclipse period is 0925-1035. (Bottom) The particle data for day 107 show a low flux of plasma sheet electrons up to 10 keV at eclipse entry. A newer population appears at 1015, coinciding with a small increase in electric field strength.
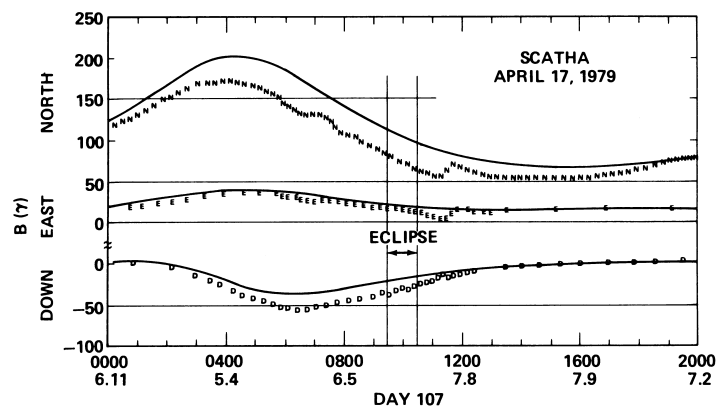
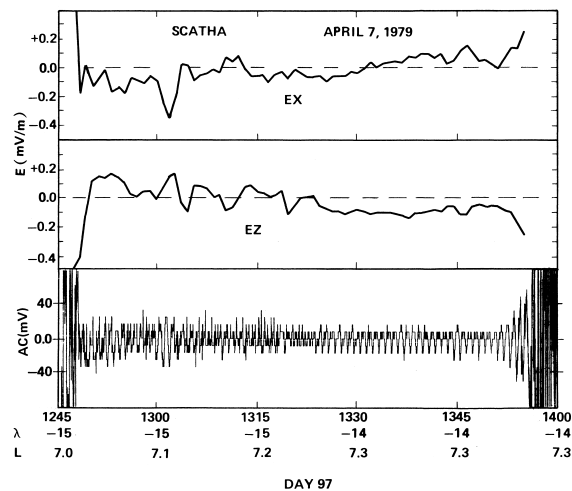Fig. 9. The magnetic field data for day 107 show a magnetic field which is almost dipolar.

Fig. 10. Electric field data for day 97, 1979.

Day 102, 1979, was a period of lower magnetic activity (Kp = 3). The electric field data for this day are plotted in the top panel of Figure 6. Here the electric field in the midnight auroral region was observed to be primarily solar-oriented and variable from 0 to 1 mV/m in the eclipse period. This time variability may be due to a Pc 5 micropulsation superimposed on a static field of similar magnitude. The satellite was outside the plasmapause in the plasma sheet during this period, as illustrated in the bottom panel of Figure 6. The Alfven layer energy was — 10 keV. The magnetic field data show the magnetic field geometry is still distorted (Figure 7). The measure of distortion adopted here, $|\Delta B|$, is 0.58, the second largest value in the analyzed data set. A 5-γ modulation is apparent with the same period as the variations in the electric field data.

Fig. 12. Electron data for day 288 of 1979 in distribution function format.

Day 107, 1979, shows a case of a weakly distorted midnight magnetosphere during a period of low magnetic activity (Kp = 2+). The satellite is still outside the plasmasphere in the plasma sheet. The electric field was about 0.1 to 0.2 mV/m during this period, as shown in the top panel of Figure 8. The particle data are shown in the bottom panel of Figure 8. The Alfven layer energy drops from 8 to 4 keV during the first hour of the eclipse period. A more intense keV electron population appears at 1015, accompanied by a modest
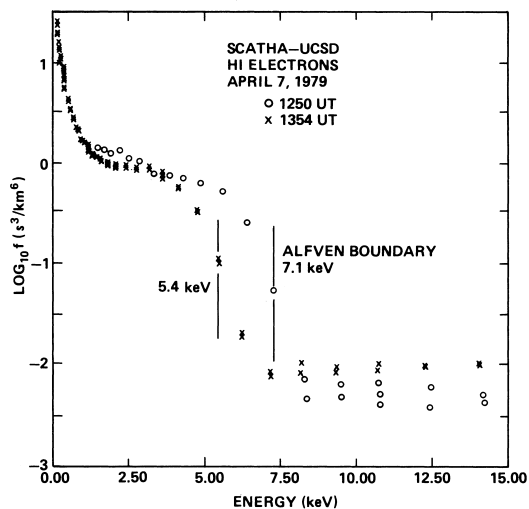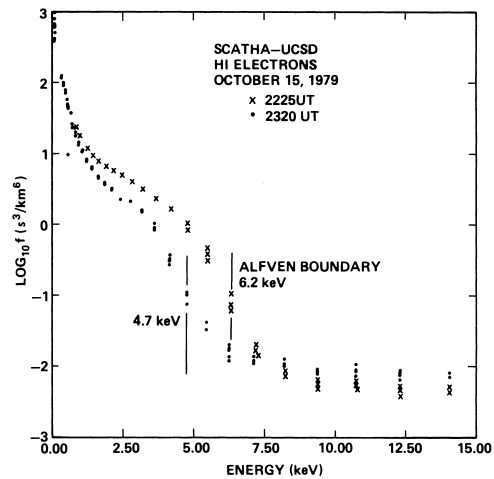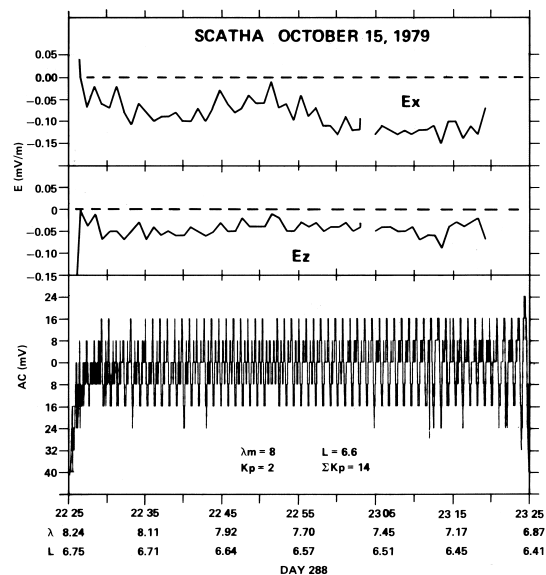

Fig. 11. Electron data for day 97 of 1979 are shown in distribution function format. The upper energy cutoff for plasma sheet electrons drops from 7 keV at eclipse entry to 5 keV at eclipse exit.

Fig. 13. Eclipse electric field data for day 288, 1979. The eclipse is from 2225 to 2315 UT. The despun (fitted) values for E,, and E show fluctuations of ±0.05 mV/m due to environmental variations and the instrument sensitivity.
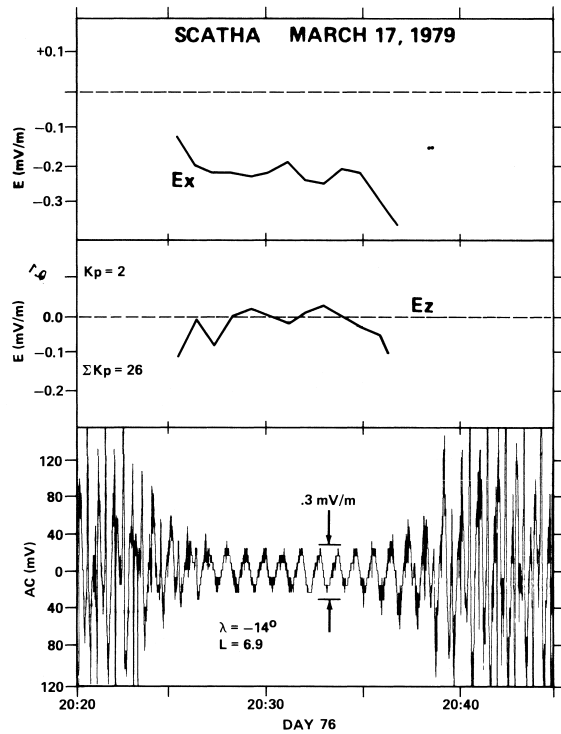
Fig. 14. Electric field data for day 76 of 1979. The penumbral eclipse is from 2025 to 2040.

increase in the electric field strength. The magnetic field is plotted in Figure 9, in topographic coordinates. The distortion measure $|\Delta B|$ is 0.27, reflecting the low Kp value.

In general, the magnitude of the electric field vector observed
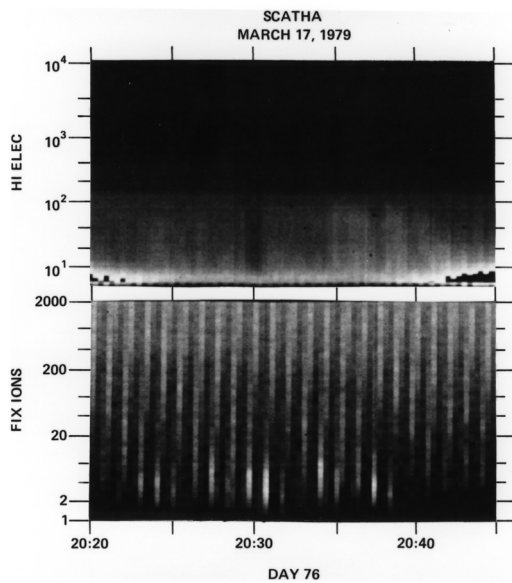

Fig. 15. Particle data for day 76 of 1979 are shown from the high energy electron detector (top panel) and fixed (low energy) ion detector.
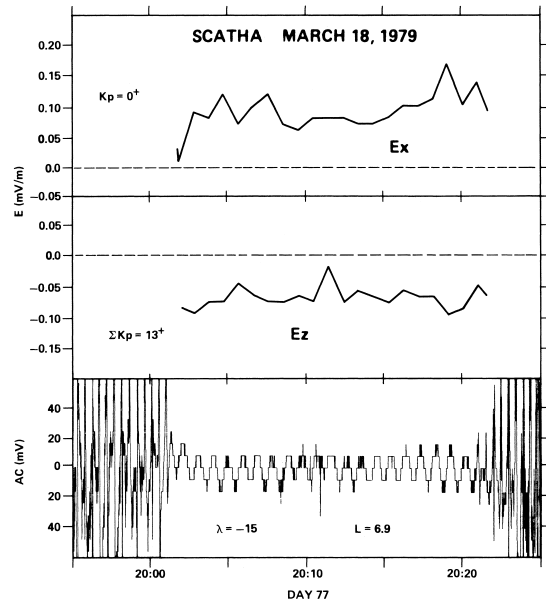

Fig. 16. Electric field data for day 77 of 1979. The eclipse is from 2002 to 2022 UT.

during magnetically average or quiet periods is quite modest at $L = 7$ in the midnight meridian. We have a number of eclipse passes similar to that shown in Figure 8. The magnitude of the electric fields is a small fraction of 1 mV/m and will map into the ionosphere with magnitudes of the order of 13 mV/m. These fields map to a latitude somewhat below the auroral oval because of the distortion of the dipole field lines in the midnight meridian. These measurements are consistent with those of *Maynard et al. [1983]*, albeit they are made under completely different probe conditions since they were made without the presence of the photoelectron sheath. After these first examples, the straightforward relationship between E and $|\Delta B|$ disappears, with $|\Delta B|$ settling between 0.2 and 0.4 and E, varying between +0.2 and -0.2 mV/m. No apparent order is imposed by the interplanetary magnetic field (IMF) either, with Bz varying from +5 γ to -1 γ in the remaining cases.

As the satellite approaches the inner edge of the plasma sheet, the radial electric field changes direction, becoming tail-ward. On day 97, 1979, the satellite crosses this boundary several times as it
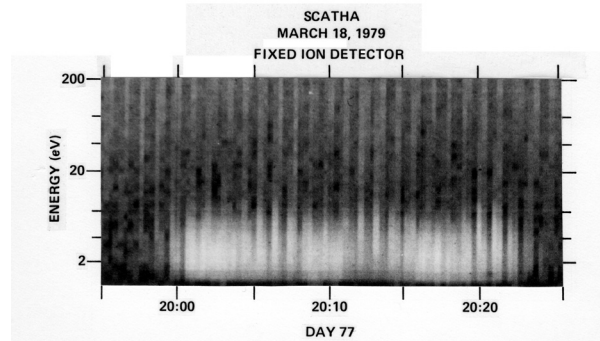

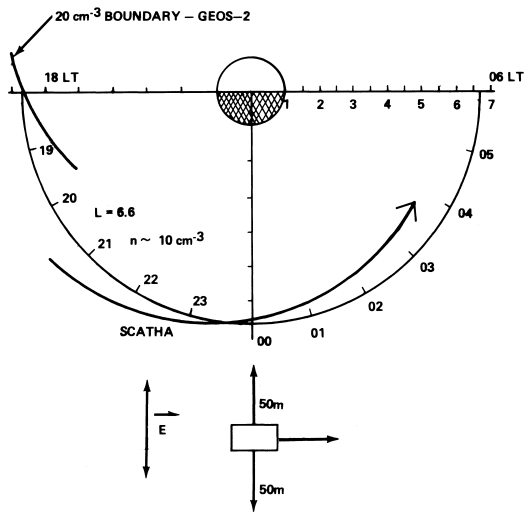Fig. 17. Fixed detector ion data for day 77 of 1979.

Fig. 18. Orbit for SCATHA on day 291 of 1979.

moves radially outward, and it crosses the midnight meridian. Figure 10 shows the electric field data in raw form and despun into SE X-Z coordinates.

Figure 11 shows the electron data as distribution functions. The satellite is in the plasma sheet, with the Alfven layer energy dropping from 7.1 keV to 5.4 keV during the eclipse. The satellite entered the plasma sheet at 1000 UT, 2000 LT, 5.5 RE. By 1300 UT the satellite is apparently crossing a boundary between eastward and westward convection of low-energy plasma (in the corotating frame).

As magnetic activity decreases, the satellite effectively moves duskward, or inward, and the electric field increases in the tailward direction. On day 288, SCATHA enters the plasma sheet 2 hours prior to eclipse, and by local midnight the Alfven layer energy is dropping from 6.2 to 4.7 keV (Figure 12). The electric field is 0.15 to 0.2 mV/m tailward (Figure 13). The magnetic field is nearly dipolar. The combination of observed electric field with the correction for satellite motion (i.e., the corotation field) results in a nearly zero net radial field. Such fields might lead to a stagnation region, such as has been suggested for the dusk bulge.

On day 76 the largest tailward field observed by SCATHA in the plasma sheet is found. Figure 14 shows a field which reaches almost 0.3 mV/m in the corotating frame, indicating a net zero field, and a plasma which is nearly stationary with respect to the earth. The particle data (Figure 15) show anisotropic low energy ions, with electron fluxes that extend only up to 200-300 eV, indicating the satellite is outside but not far from the plasmasphere.

The magnitude of the electric fields (0-2 mV/m) we have shown for satellite eclipse periods in the plasma sheet and the dependence of the observed magnitude on magnetic activity are similar to the previous observations from the ISEE 1, GEOS 1, and GEOS 2 satellites referenced earlier. These observations provide a framework for understanding our unique observations of the electric field at the edge of the plasmasphere.

Eclipse Electric Fields in the Plasmasphere

It might have been expected that there would be little or no electric field in the plasmasphere, other than the corotation field. Maynard et al. [1983] showed, however, that the convection fields penetrate into the plasmasphere during periods of high activity. One example of such fields is the sunward field found in the plasmasphere on day 77. SCATHA is at 6.1 RE, L = 6.9. Figure 16 shows the 0.1- to 0.2-mV/m field. Figure 17 shows the appearance of cold, isotropic ions as SCATHA is eclipsed, with a field-aligned ion population superimposed. This plasma, particularly the isotropic portion, has been termed a "hidden" ion population [Olsen, 1982]. These measurements are made possible by a drop in the spacecraft potential, to near 0 V. GEOS 2 is in conjunction with SCATHA at this time, and the active sounder reports a plasma density of 70 cm^{-3} at L = 6.7 and a plasmapause at 0100 LT (P. M. E. Decreau, personal communication, 1984) [Olsen et al., 1983]. The addition of GEOS data shows that SCATHA is just inside the plasmapause. This plasma is apparently "superrotating," i.e., flowing eastward at a velocity greater than the corotation velocity.

Electric Fields at the Plasmapause

One of the major motivations for this work was to deter-mine if there was a discontinuity in the radial electric field at the plasmapause. Here, a discontinuity means a variation in the electric field on the same time scale as the plasmapause crossing, typically 10-100 s as shown by the particle data. Two plasmapause examples were found in the 1979 eclipse data set.

Day 291 (October 18, 1979) is one of a series of days studied for a GEOS-SCATHA conjunction paper [Olsen et al., 1983]. The addition of GEOS data provides absolute densities and a slightly different measurement location to aid in determining the plasmapause location. GEOS 2 left the plasmasphere near local dusk, at 6.6 RE, crossing the 20 cm-3 boundary at 1800 LT. GEOS was outside the plasmasphere at local midnight, at 6.6 RE, while SCATHA shows a plasmapause structure near L = 6.5 at 2141 UT. The satellite locations and SCATHA orientation are illustrated in Figure 18. This is the one case of southward IMF in this data set. The IMF turned south at ISEE 3 at 1930 UT and was −3 γ from 2000 to 2100 UT.

Figure 19 shows the particle data for day 291 in 1979. The eclipse period begins on day 291 at 2120. The "hidden" ion population which is the plasmasphere plasma is evident on entrance into the eclipse. Beginning at approximately 2145 this low-energy ion population becomes striated, and a clear crossing into the plasma sheet electron population is evident. The signature of the plasma sheet electrons is the slow in-crease of the cutoff energy beginning at 20 eV at 2155, 80 eV at 2205, and 200 eV upon exit of the eclipse at 2225.

Plotted in Figure 20 are the electric field data. This electric field is in the antisolar direction. It begins at 0.05 mV/m in the plasmasphere and builds in strength to 0.3 mV/m as the cutoff energy of the plasma sheet electrons increases. Aside from the brief increase at 2141 (see below) it is clear from Figure 20 that this radial electric field is near zero in the plasmasphere and builds up in a nonsingular fashion as the satellite enters the plasma sheet.
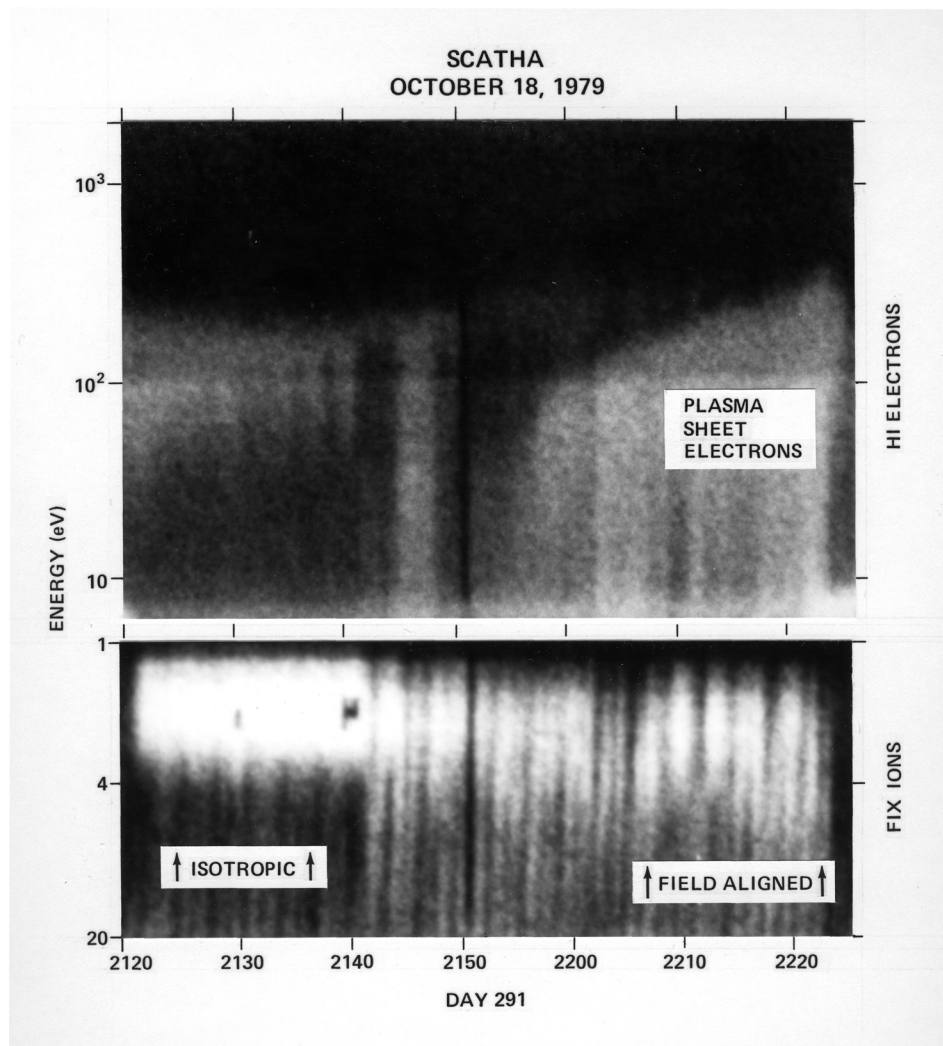
Fig. 19. Particle data for day 291 of 1979 are shown for the high-energy electron detector and fixed ion detectors.

The plasmasphere is corotating with the earth, and the plasma sheet population is convecting toward the dusk meridian (in earth-fixed or synchronous inertial coordinates). This dependence of the radial electric field is not unexpected; most plasmasphere theoretical studies suggest similar electric field variations with a corotating plasmasphere.

The electric field measured at 2141 is shown in detail in Figure 21. The transient nature of these fields is clear. There is no perceptible variation in the magnetic field data, so we infer this is not a temporal variation in the environment. It may be that this is the result of a modest charge buildup at the plasmapause. If so, this would be our "discontinuity," a transient field of 0.1 to 0.2 mV/m. The steady state field measured in the plasma sheet is shown in Figure 22. These data represent a digital version of a sine wave and

illustrate the cleanliness of the measurements which can be obtained in eclipse.

Finally, Figure 23 shows plasma data for 3 hours on October 19, 1979, including the eclipse period from 2100 to 2206 UT (shown previously by *Olsen [1982]*). The eclipse period in this panel can be readily recognized by the disappearance of the photoelectron at low energies and the intensification of the observed fluxes of low-energy ions. No injections of hot plasma from substorm events occurred in the 12 hours prior to this eclipse period. The plasma sheet electrons extend up to 1 keV at 2000 UT. This cutoff energy decreased steadily until 2120 UT, when the plasma sheet electrons disappear. The ion fluxes shown in Figure 23 show the vertical striping signature of a field-aligned pitch angle distribution early in the eclipse,
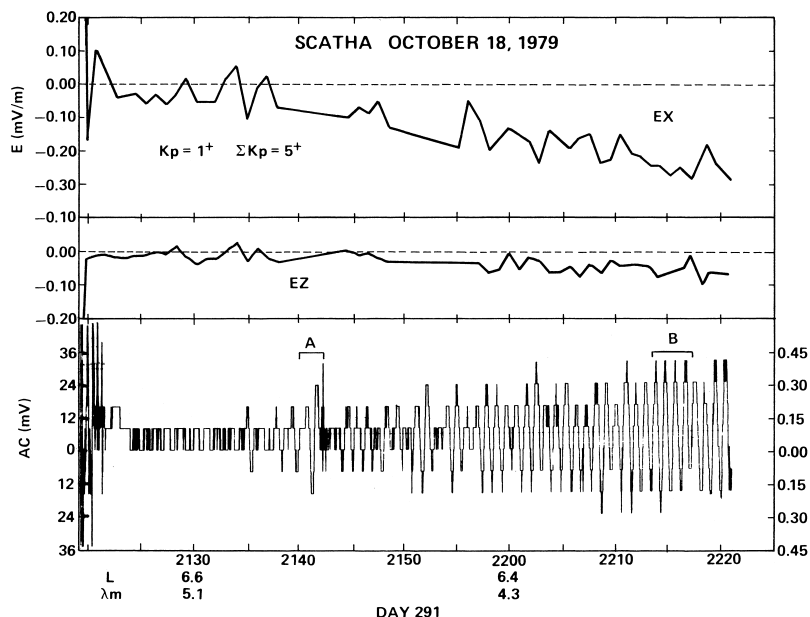
Fig. 20. Electric field data for day 291 of 1979. The eclipse is from 2120 to 2227.

in the plasma sheet. As the plasma sheet electrons disappear, a striking solid white region appears which is the low-energy isotropic ion population of the plasmasphere. Thus the plasmapause was crossed twice during the eclipse period, entering the plasmasphere at 2120 and leaving it at 2150.

Figure 24 shows the electric field data for this eclipse period on day 292, 1979. There is only a trace of electric field (<0.1 mV/m) evident in the plasma sheet during this eclipse period. The amplitude falls even lower in the plasmasphere, to a value that cannot be resolved by the telemetry resolution (12/256 mV/m or 0.05 mV/m). The direction of this small electric field vector in the X-Z plane was antisunward or northward in the northern projected ionosphere. The amplitude of this electric field during this encounter with the plasmapause is so small that only the direction is clear. Clearly, there are no sharp discontinuities at this boundary.
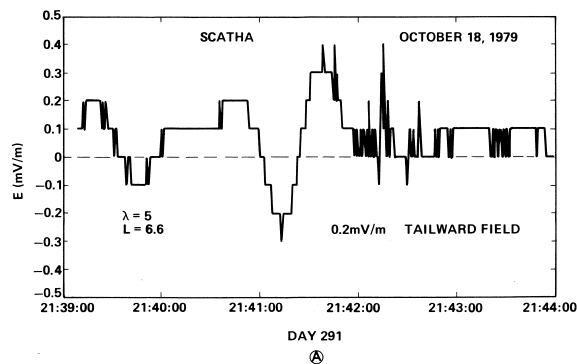
SUMMARY AND DISCUSSION

We have reported static electric field measurements in the near-equatorial plane from the 100-m double floating probe experiment carried on the SCATHA P-78-2 satellite. These measurements may be quite significant in furthering our understanding of the formation of the plasmasphere. Eclipse measurements on auroral L shells show a very definite correlation with the plasmapause and the plasma sheet structure at low magnetic activity. The use of eclipse data allows the electric fields to be measured directly without contamination from the satellite photoelectron sheath, and its use allows the thermal ion population in the plasmasphere to be observed at low energies.

We have found that, in general, there is an electric field component in the radial outward direction at low magnetic activities that begins at the edge of the plasmasphere and that builds in amplitude as the satellite enters the plasma sheet. The amplitude of this electric field vector varies from 0.05 to 2 mV/m and reverses in sign with increasing magnetic activity. The structure of these fields is summarized by Figure 25, in an inertial reference frame.
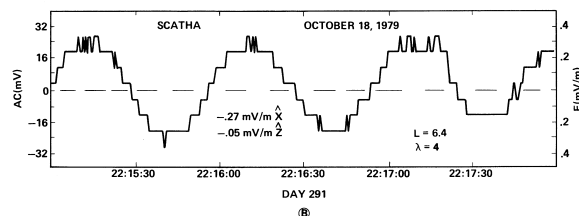

Fig. 21. Plasmapause electric field.

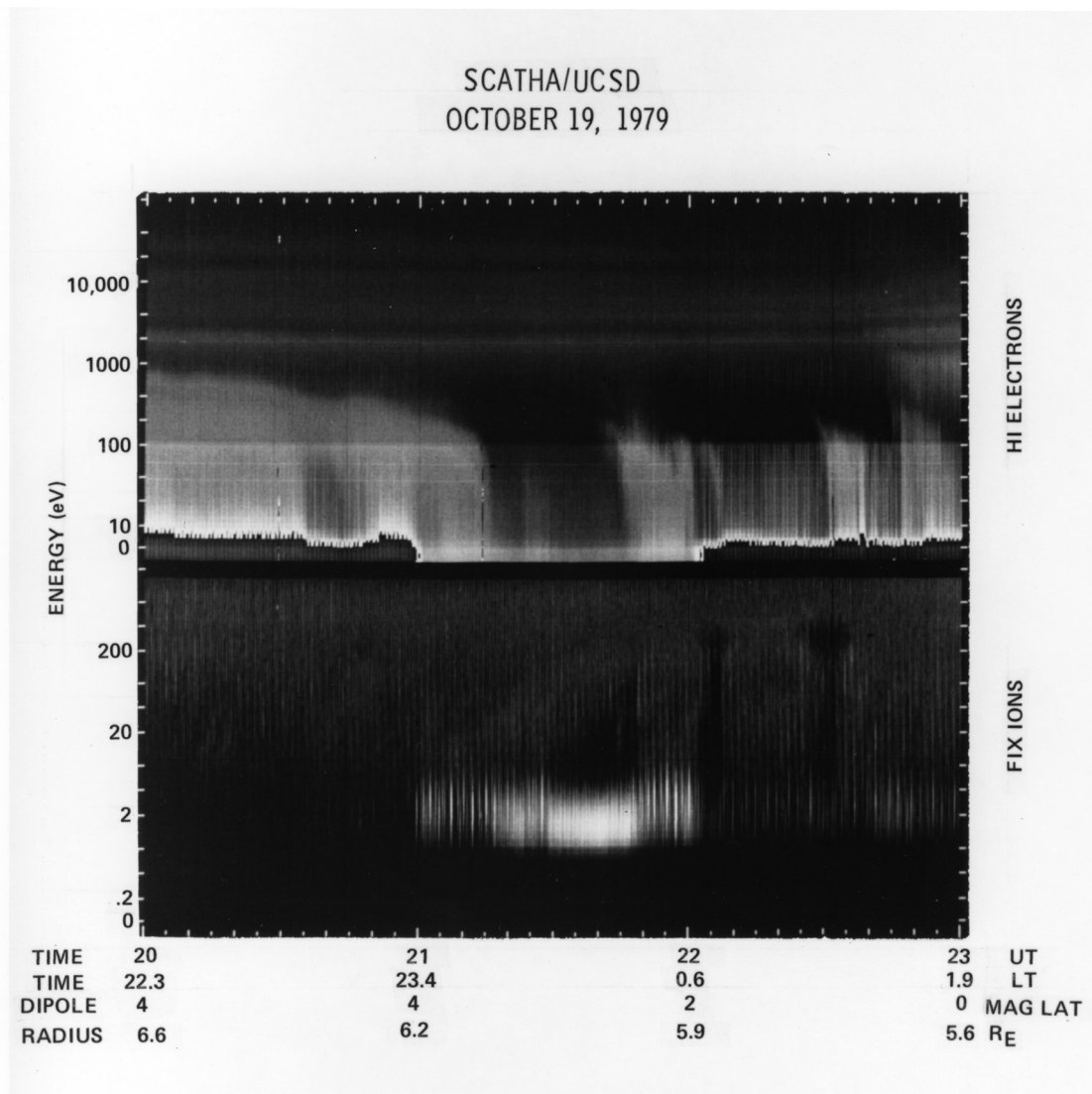Fig. 22. Plasma sheet electric field data.

Fig. 23. Spectrogram for ions and electrons on day 292 of 1979.

The ensemble of data considered so far suggest that during more active periods (i.e., when SCATHA has penetrated further into the plasma sheet), the fields are initially near zero and then become sunward, increasing in amplitude with magnetic activity. Since our measurements are all at local midnight, it is inferred that the pattern in Figure 25 rotates through local midnight as magnetic activity varies. These fields indicate a stagnation region near the plasmapause, toward local dusk.
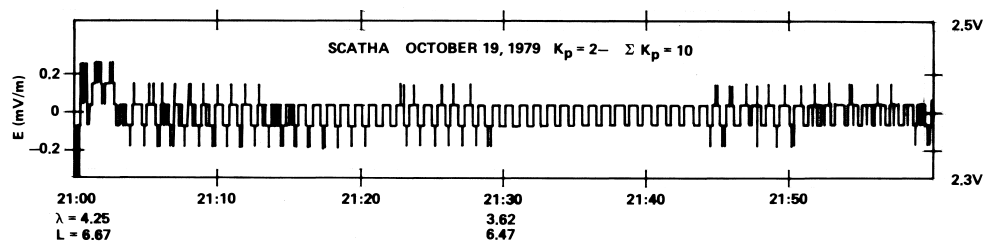

Fig. 24. Electric field data for day 292 of 1979. The eclipse is from 2100 to

SUMMARY OF SCATHA ELECTRIC
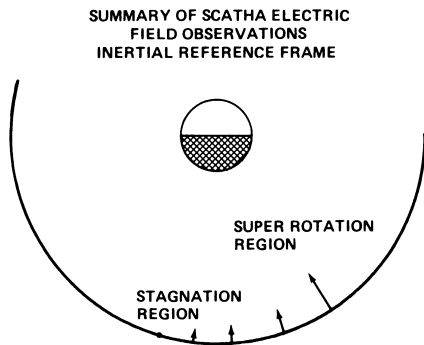FIELD OBSERVATIONS
INERTIAL REFERENCE FRAME

Fig. 25. Summary of SCATHA eclipse observations.

The amplitude of the observed electric field also is shown to increase with the amount of distortion in the magnetic field vector at the satellite from the cross-magnetotail current system. During one plasmapause crossing, a transient tailward field of 0.2 mV/m appeared. There is not, however, a sharp discontinuity in the convection fields at the plasmapause; in-stead, the shielding of the plasmasphere is gradual, allowing the convection fields to penetrate into the plasmasphere.

The direction of the observed electric field vector is only known in the solar ecliptic X-Z plane (the spin plane of the SCATHA satellite). The east-west component of electric field is not measured during these eclipse events. However, since the plasmapause boundary and the plasma sheet boundary are known to lie in the E-W direction and since these boundaries are clearly tangential discontinuities, we strongly suspect that the E-W component of E is small during these events, or at least slowly varying.

These observations can be compared to standard models of the plasmapause structure, such as the one derived by Kavanagh et al. [1968] which we have illustrated in Figure 26. Kavanagh et al. defined the plasmapause as the boundary between plasma corotating with the earth and plasma convecting from the tail toward the sun under the influence of a dawn-to-dusk electric field of the order of 0.5 mV/m. Figure 26 is a plot of equatorial plane equipotentials of streamlines of flow according to these assumptions, and the plasmapause is taken to be the last closed equipotential, shown as a solid line in Figure 26.

An arrow drawn in the antisolar direction in the midnight meridian would cross an enhanced region of potential con-tours just outside the plasmapause in Figure 26. This might appear as an abrupt rise of the antisolar electric fields during the passage through the plasmapause. Such variations are not observed during our plasmapause crossings, such as the examples illustrated by Figures 20 and 24. Further comparison requires that we again note that the electric fields observed with SCATHA are measured in a near-corotating system since the satellite is in a near-synchronous orbit. The equipotential contours shown in Figure 26 are drawn for a noncorotating system. Indeed, the electrostatic contours plotted in Figure 26 correspond to (1) corotating electric fields and (2) a dawn-todusk electric field perpendicular to the midnight meridian. Neither of these electric fields would contribute significantly to our observations of radially outward electric fields in the mid-night meridian with a satellite corotating with the earth's rotation. These considerations apply strictly only to the model of

EQUATORIAL PLANE ELECTRIC EQUIPOTENTIALS
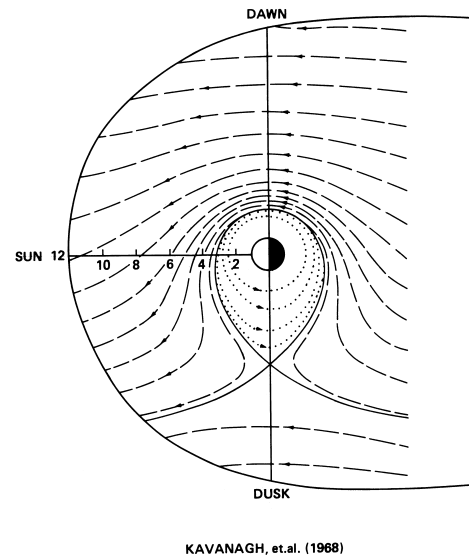

KAVANAGH, et.al. (1968)

Fig. 26. Equatorial electric potentials or streamlines of flow according to Kavanagh et al. [1968]. The plasmapause is taken to be the last closed equipotential shown as a solid line.

Kavanagh et al. [1968], but they also apply to most models of the structure of the plasmapause.

In the recent computer models of magnetospheric convection which have been simulated at Rice University [Hare! et al., 1981; Spiro et al., 1981], a small radial electric field might exist because of the small canting of the applied east-west electric field as a function of increased magnetic activity. However, in these models the midnight meridian is essentially a null line for the radial electric fields in the midnight meridian.

As an alternate approach to identifying the origin of the electric field which we have observed to correlate with the structure of the plasmapause, consider the effect of the inner magnetosphere corotating through the ring current/cross-tail currents in the midnight meridian. The east-west currents in the plasma sheet cause the observed distortions in B noted for each example, and the larger electric fields were associated with the more distorted magnetic fields. A radial electric of the order of $E_r = \omega \times r \times Bm$ could be created. Here Bm is the contribution from the standing current system near the mid-night meridian, ω the rotation velocity, and r the radial distance. Such an electric field would be of the order of 0.1 mV/m for a 30-γ contribution from the tail-related current system. This magnitude is probably too small to explain our observations.

REFERENCES

Aggson, T. L., B. G. Ledley, A. Egeland, and I. Katz, Probe measurements of DC electric fields, Proceedings of the 17th ESLAB Symposium, on `Spacecraft/Plasma Interactions and Their Influence on Field and Particle Measurements', Noordwijk, The Netherlands, 13—16 September 1983, *Eur. Space Agency Spec. Publ.*, ESA SP-198, 13, 1983a.

Aggson, T. L., J. P. Heppner, and N. C. Maynard, Observations of large magnetospheric electric fields during the onset phase of a substorm, *J. Geophys. Res.,* 88, 3981, 19836.

Carpenter, D. L., Whistler studies of the plasmapause in the magnetosphere, *J. Geophys. Res.*, 71, 693, 1966.

Chappell, C. R., K. K. Harris, and G. W. Sharp, A study of the influence of magnetic activity on the location of the plasmapause as measured by OGO 5, *J. Geophys. Res.*, 75, 50, 1970.

DeForest, S. E., and C. E. McIlwain, Plasma clouds in the magnetosphere, *J. Geophys. Res.*, 76, 3587, 1971.

Harel, M., R. A. Wolf, P. H. Reiff, R. W. Spiro, W. J. Burke, F. J. Rich, and M. Smiddy, Quantitative simulation of a magnetospheric substorm, 1, Model logic and overview, *J. Geophys. Res.*, 86, 2217, 1981.

Heppner, J. P., E. A. Bielecki, T. L. Aggson, and N. C. Maynard, Instruments for DC and low-frequency electric field measurements on ISEE-A, *IEEE Trans. Geosci. Electron.*, GE-16, 253, 1978a.

Heppner, J. P., N. C. Maynard, and T. L. Aggson, Early results from ISEE-1 electric field measurements, *Space Sci. Rev.*, 22, 777, 19786.

Horwitz, J. L., W. K. Cobb, C. R. Baugher, C. R. Chappell, L. A. Frank, T. E. Eastman, R. R. Anderson, E. G. Shelley, and D. T. Young, On the relationship of the plasmapause to the equatorward boundary of the auroral oval and to the inner edge of the plasma sheet, *J. Geophys. Res.*, 87, 9059, 1982.

Kavanagh, L. D., Jr., J. W. Freeman, Jr., and A. J. Chen, Plasma flow in the magnetosphere, *J. Geophys. Res.*, 73, 5511, 1968.

Mauk, B. H., and C. E. McIlwain, ATS6 UCSD auroral particles experiment, *IEEE Trans. Aerosp. Electron. Syst.*, AES-11, 1125, 1975.

Maynard, N. C., Electric field measurements across the Harang discontinuity, *J. Geophys. Res.*, 79, 4620, 1974.

Maynard, N. C., and J. M. Grebowsky, The plasmapause revisited, *J. Geophys. Res.*, 82, 1591, 1977.

Maynard, N. C., T. L. Aggson, and J. P. Heppner, The plasmaspheric electric field as measured by ISEE 1, *J. Geophys. Res.*, 88, 3981, 1983.

McIlwain, C. E., Plasma convection in the vicinity of geosynchronous orbit, in *Earth's Magnetospheric Processes*, edited by B. M. McCormac, p. 268, D. Reidel, Hingham, Mass., 1972.

Moe, T. E., N. C. Maynard, and J. P. Heppner, Micropulsations in the electric field near the plasmapause observed by ISEE, *J. Geophys. Res.*, 85, 2099, 1980.

Mozer, F. S., R. B. Torbert, U. V. Fahleson, C: G. Falthammar, A. Gonfalone, and A. Pedersen, Electric field measurements in the solar wind, bow shock, magnetosheath, magnetopause, and magnetosphere, Space Sci. Rev., 22, 791, 1978.

Olsen, R. C., The hidden ion population of the magnetosphere, *J. Geophys. Res.*, 87, 3481, 1982.

Olsen, R. C., A threshold effect for spacecraft charging, *J. Geophys. Res.*, 88, 493, 1983.

Olsen, R. C., P. M. E. Decreau, J. F. E. Johnson, G. L. Wrenn, A Pedersen, and K. Knott, Comparison of thermal plasma observations of SCATHA and GEOS, Proceedings of the 17th ESLAB Symposium, on `Spacecraft/Plasma Interactions and Their Influence on Field and Particle Measurements', Noordwijk, The Nether-lands, 13—16, September 1983, *Eur. Space Agency Spec. Publ.*, ESA SP-198, 57, 1983.

Pedersen, A., and R. Grard, Quasistatic electric field measurements on the GEOS-1 and GEOS-2 satellites, in *Quantitative Modeling of Magnetospheric Processes*, Geophys. Monogr. Ser., vol. 21, edited by W. P. Olson, p. 281, AGU, Washington, D. C., 1979.

Pedersen, A., R. Grard, K. Knott, D. Jones, A. Gonfalone, and U. Fahleson, Measurements on quasi-static electric fields between 3 and 7 earth radii on GEOS-1, *Space Sci. Rev.*, 22, 333, 1978.

Pedersen, A., C: G., Falthammar, V. Formisano, P: A. Lindquist, F. Mozer, and R. Torbert, Quasi-static electric field measurements with spherical double probes on the GEOS and ISEE satellites, *Space Sci. Rev.*, 37, 269, 1984.

Spiro, R. W., M. Harel, R. A. Wolfe, and P. H. Reiff, Quantitative simulation of a magnetospheric substorm, 3, Plasma electric fields and evolution of the plasmapause, *J. Geophys. Res.*, 86, 2261, 1981.

Taylor, H. A., H. C. Brinton, and M. W. Pharo, Contraction of the plasmasphere during geomagnetically disturbed periods, *J. Geophys. Res.*, 73, 961, 1968.

Wolf, R. A., Ionosphere-magnetosphere coupling, Space Sci. Rev., 17, 537, 1975.

T. L. Aggson and B. G. Ledley, NASA Goddard Space Flight Center, Greenbelt, MD 20771.

R. C. Olsen, Department of Physics, University of Alabama, Huntsville, AL 35899.